

電気化学反応に伴う金属電極表面形態変化と物質移動速度の連結現象と重力レベル効果

若月 孝夫，有瀬 一郎，大崎 博史（京大），本間 敬之，福中康博（早大）

Gravitational Level Effects on Coupling Phenomena between Morphological Variations of Electrode Surface and Ionic Mass Transfer Rate

Takao Wakatsuki, Ichiro Arise*, Hiroshi Osaki*, Takayuki Homma**, and Yasuhiro Fukunaka***
*Kyoto University, Kyoto, Kyoto 606-8507
**Waseda University, Shinjuku, Tokyo 169-8555
E-Mail: fukunaka@aoni.waseda.jp

Abstract: A horizontal upward-facing Zn anode was electrochemically dissolved in aqueous alkaline electrolyte. A plane-parallel upward facing $Ni(OH)_2$/NiOOH cathode was combined with the Zn anode in a single cell. This configuration can be regarded as a single pore model inside the porous space of a Zn-NiOOH battery cell. It also insures that the ionic mass transfer rate by diffusion and migration mechanism is dominant over that by natural convection. The morphological variations of the Zn anode surface were examined during the discharge operation. Two-dimensional transient concentration profiles of each ion accompanying the electrochemical dissolution of Zn anode in alkaline electrolyte were numerically calculated. The surface morphological variations of the Zn anode were discussed based on the coupling phenomena. ZnO precipitation on the Zn anode surface was confirmed to be dependent on the horizontal distance from the separator. The present numerical model provides insight to the analysis of observed morphological variations along the Zn anode surface. Such a research may provide a more profound understanding on Li battery operation in space environment as well.
Key words; Energy Conversion & Storage, Coupling Phenomena, Battery Reversibility, Dendrite

1. Introduction

URFC and Li battery are the key devices as well as Life Supporting system in Space Exploration toward to Mars. Electrochemical interfacial phenomena must play the most important role in these devices. The gravitational level effect to the electrochemical processes like water electrolysis and secondary batteries was examined in JAMIC Drop Tower. Ni-Zn battery was installed on the top of capsule. After dropping the capsule in the shaft, the charging operation of battery was indispensable. It provided us a strong impact how important the energy conversion & storage devices are in the space exploration as well as the movie, “Apollo the 13th”.

Rechargeable batteries for electric vehicle (EV) and hybrid electric vehicle (HEV) applications have been a subject of intense focus for the last decade or so. Although Li-based systems have received the most attention, there has been increasing interest in Zn-based systems because of their lower costs, material abundance, and compatibility with nonflammable aqueous electrolytes. Zn anode morphological variations however introduce some serious problems of short life, poor reliability, and safety issues. The coupling phenomena between ionic mass transfer rates and electrode surface morphological variations must be well understood. The goal is to incorporate the fundamental knowledge of Zn electrochemical processes into a numerical model for a hybrid electric vehicle (HEV) battery as well as large-scale battery operation.

It is of practical importance to predict the cell voltage and current distribution of a battery for vehicle applications with a numerical model, as an aid to the design of an electric control unit (ECU). Therefore, this paper first describes the physical model pore simulation considering only diffusion and electrophoresis mechanisms. An electrochemical cell with a horizontal upward-facing Zn anode nearby a plan-parallel $Ni(OH)_2$/NiOOH electrode has been used frequently in order to suppress the natural convection induced by buoyancy forces.

2. Experimental

The experimental apparatus is drawn in Figure 1. Briefly, an

electrochemical cell was fabricated from an acrylic plate, and a 99.99% zinc plate was used as the working electrode. The $Ni(OH)_2$/NiOOH counter electrode was charged to 50–80% state of charge before cell discharge. This configuration was adopted to suppress the natural convection driven by buoyancy forces. In the present work, a polyolefin separator is placed between the negative and positive electrodes. The $[Zn(OH)_4]^{2-}$ ions are blocked by the separator surface adjacent to Zn electrode because of the larger size of the $[Zn(OH)_4]^{2-}$ ions compared to OH^- and K^+ ions. Certainly, such an assumption would not be valid in a practical cell after many cycles or an extended cell charge or discharge, but it should be a good approximation for a short-duration experiment. The tip of a Hg/HgO reference electrode was positioned about 3 mm from the Zn working electrode. Galvanostatic electrolysis was carried out in a 1.95 M KOH (10% by weight KOH) aqueous electrolyte at 293 K. The concentration of KOH aqueous electrolyte is lower than most commercial alkaline electrolyte(30–40% by weight KOH), and is purposely chosen because it is easier to measure the zincate concentration distribution at lower OH^- ion concentrations.

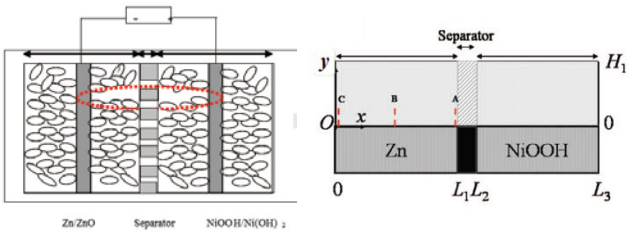

Figure 1

3. Results & Discussion

The surface morphological variations of Zn anode were examined. The electrochemical dissolution of the Zn anode was carried out over various periods after starting the galvanostatic electrolysis at the average applied current densities of i_{ave} = 20 and 40 mA/cm2 (HA-305 galvanostat, Hokuto Denko LTD.). The electrolysis duration time was determined with the aid of numerical simulation. Each electrode was freshly prepared before electrochemical testing. The discharged electrode was removed from the electrochemical cell and rinsed with ethanol. Three points on the Zn anode surface were selected for SEM observation: adjacent to the separator, the center of electrode, and near the current collector wire.

Physical and Mathematical Modeling

During the discharge of Zn-NiOOH batteries, OH^- is consumed on the Zn electrode surface, as expressed by the equation 1

$$Zn + 4OH^- = Zn(OH)_4^{2-} + 2e^- \quad [1]$$

The electrochemical reaction on NiOOH electrode can be also expressed as follows.

$$NiOOH + H_2O + e^- = Ni(OH)_2 + OH^- \quad [2]$$

Eq. 1 does not *a priori* involve the dissolution-precipitation mechanism of $[Zn(OH)_4]^{2-}$ ions and ZnO. When the $[Zn(OH)_4]^{2-}$ ions concentration on the anode surface exceeds the chemical solubility limit or the electrochemical solubility limit, the precipitation of ZnO or $Zn(OH)_2$ may take place, which can be written by the following chemical reaction equation.

$$Zn(OH)_4^{2-} = ZnO + 2OH^- + H_2O \quad [3]$$

$$Zn(OH)_4^{2-} = Zn(OH)_2 + 2OH^- \quad [4]$$

The holographic interferometry technique might provide such information at a geometrically flat electrode surface. Once the surface becomes rough with hydroxide precipitation, interferometry may lose the capability to monitor the transient behavior of two-dimensional refractive index profiles disturbed by the surface roughness as well as by the heterogeneous reactivity at the Zn anode surface along an optical path. Thus, *ex situ* observation of surface morphology for Zn anode is presented and discussed in combination with the numerical simulation in this study.

Transient mass transfer rates of both $[Zn(OH)_4]^{2-}$ and OH^- ions during discharge operation of Zn-NiOOH cell in a 1.95 M KOH aqueous electrolyte are numerically analyzed. Three regions can be identified: Zn electrode compartment, polyolefin separator compartment, and NiOOH electrode compartment. The governing electrolyte-phase equations in each compartment can be expressed as follows according to mass conservation and electroneutrality equations under the assumption of constant physical properties.

Both anodic and cathodic current density distributions are calculated along the electrode surface. The Zn anode surface

overpotential η_s can be expressed according to the Butler-Volmer equation. The anode surface overpotential can be calculated by using the constraint condition that the integration of local current density over the electrode surface area must be equal to the applied constant overall electrolytic current *I*. The present numerical model does not consider the electrode shape change due to both the dissolution of Zn and the precipitation of ZnO during electrolysis. Therefore, the electrode surface is assumed to be perfectly flat during the numerical simulation. The above-described 2D mathematical model was solved numerically by using the finite differences method and deterministic relaxation techniques.

Figure 2 shows the transient variation in calculated anode surface concentrations of both $[Zn(OH)_4]^{2-}$ and OH^- ions at x = 0.1, 4, and 7.9 mm along the Zn anode at i_{ave} = 20 mA/cm^2 in 1.95 M KOH electrolyte. The concentrations of zincate ion and hydroxide ion are nearly identical for x = 0.1 and x = 4 because the influence of hydroxide ion concentration changes at the positive electrode is small at $0<x\leq 4$.

Before carrying out ex situ SEM observations, the forming process of the black ZnO or $Zn(OH)_2$ film was observed in situ by the naked eye as the electrolysis progressed, and the disappearance of the black ZnO or $Zn(OH)_2$ film was observed when current was reversed. It was observed that this film delaminated from the anode surface due to the hydrodynamic drag force accompanying the evolution of O_2 gas bubbles. The interference fringe pattern images accompanying gas evolution were reported elsewhere. These naked-eye observations of electrode surface phenomena support a growth mechanism of ZnO films formed by the aggregation of hydroxide precipitates.

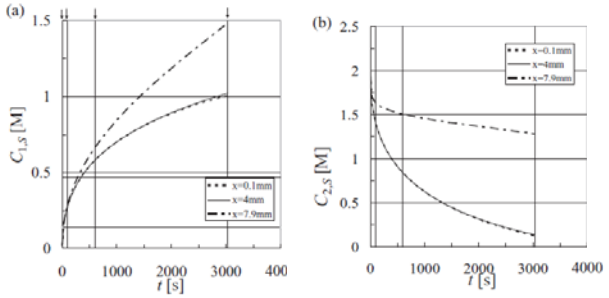

Figure 2

Our *ex situ* SEM observation results are now described. During our experiments, the chemical solubility limit of zincate ion is reached within 30 seconds and the electrochemical solubility limit is reached within 360 seconds, according to our numerical simulation model. A 5-second dissolution time after starting the galvanostatic electrolysis at i_{ave} = 20 mA/cm^2 was selected in order to observe the time variation of $Zn(OH)_2$ or ZnO precipitation in its initial stage. The $Zn(OH)_4^{2-}$ ion surface concentration should not exceed its chemical solubility limit at 5 seconds, and should remain between its chemical solubility limit and its electrochemical solubility limit at 100 seconds.

Our numerical calculation predicts that the anode surface concentration of $Zn(OH)_4^{2-}$ ion reaches 1 M (about twice the electrochemical solubility limit) over the entire Zn anode at about 3030 seconds (50.5 minutes) far away from the separator, and therefore the electrolysis was interrupted at that time. In practice, 15240 seconds (254 minutes) was selected as the cutoff because the anode potential abruptly shifted toward the noble direction for the discharge reaction. This phenomenon arises when the surface reaction area of the zinc electrode becomes completely covered with zinc oxide.

Because the present numerical model does not include the dissolution-precipitation mechanism of ZnO, the concentration of $Zn(OH)_4^{2-}$ ion continuously increases with time. The anode surface concentration of $Zn(OH)_4^{2-}$ ion at x = 8 mm is about 1.5 times higher than that at x = 0 mm at t = 50.5 min. The figure clearly shows the depletion of OH^- ion in the Zn anode compartment and the accumulation of OH^- ion in the NiOOH cathode compartment, respectively. At about 50.5 minutes, the numerical simulation without the dissolution-precipitation mechanism of ZnO predicts the concentration of OH^- ion decreasing to less than 0.2 M, in the region ($0<x<6$ mm) away from the current collector. This result suggests that OH^- ions are transferred from the NiOOH compartment toward the Zn compartment, even though the mass transfer coefficient is small in the separator region. In addition, the concentration profiles in the vicinity of separator. In the separator, the concentration difference reaches more than 0.5M at t = 50.5 minutes, which means that the OH^- ion can be transferred not only by voltage

differences but also by concentration differences.

Figure 3 shows the morphological variations at x = 7.9 mm. Comparison with the initial Zn substrate indicates that the electrochemical dissolution reaction has slightly changed the anode surface after only 5 seconds, although many native polishing scratches ranging from 1 to 5 μ m in width still remain. Some local aggregations (probably composed of zinc hydroxide) have formed. A Zn anode dissolves into KOH aqueous solution to form the $Zn(OH)_4^{2-}$ complex ion, which begins to flocculate once the solubility product has locally exceeded the critical value at a particular site on the Zn anode. Magnified SEM images clearly demonstrate the appearance of typical quadrangular crystals. However, the calculated anode surface concentration of $Zn(OH)_4^{2-}$ ion at t = 5 seconds and i_{ave} = 20 mA/cm^2 is still below the chemical solubility limit. Thus, the appearance of hydroxide aggregations suggests a nonuniform current density distribution caused by heterogeneous surface activity of zinc anode. Another mechanism may be related to local variations in surface kinetics of the hydroxide phase nucleation phenomena at the zinc anode.

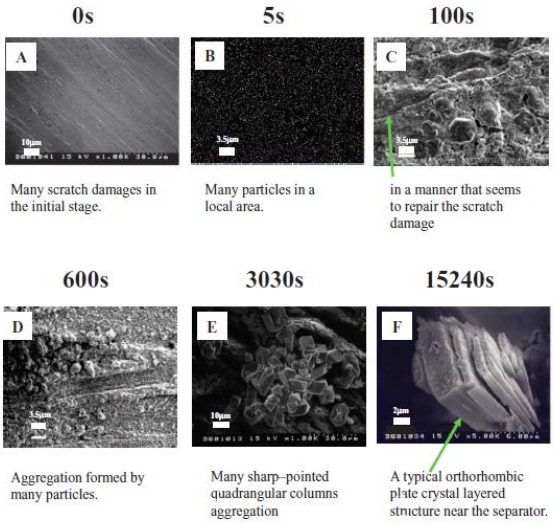

Figure 3

Hydroxide is preferentially precipitated at specific active areas. As time progresses, the precursors of quadrangular crystals begin to grow into a film. These spherical particles are initially less than 1 μ m in size, and then grow gradually to form rectangular parallelopiped precipitates along the ridge-like lines of polishing scratches. In the early stages of Zn surface oxidation, it is lightly covered with a thin and densely packed layer of many ZnO or $Zn(OH)_2$ small particles. The OH^- ion in the bulk electrolyte easily diffuses to the surface of the Zn electrode from the NiOOH electrode through the separator because the OH^- ion is very small. Zincate ion also diffuses through the interparticle space in this thin layer. Its calculated surface concentration under the presumption of no ZnO precipitation has exceeded the electrochemical solubility. This layer is thus expected to be an important determinant of battery charging and discharging rates.

A fibrous network or porous morphology of hydroxide precipitation is formed in the next stage. Furthermore, the morphology of the hydroxide precipitate develops a typical quadrangular column at t = 15240 seconds. SEM images clearly demonstrate the appearance of a typical orthorhombic plate crystal layered structure near the separator. Some mossy types of precipitations are also observed between these quadrangular columns.

4. Conclusions

The morphological variations of Zn hydroxide or Zinc oxide precipitates on Zn anode surface were examined. The transient concentration profiles of each ion accompanying the discharge operation of Zn/NiOOH cell in an alkaline solution were calculated with a two-dimensional model. Observed morphological variations on the Zn electrode qualitatively agree with the predictions. Such a methodology may be applied to the dendritic growth process in Li battery as well. ESA-ITT team “Electrochemical Nucleation & Growth”(PI: Prof. M. Rosso, Ecole Polytechnique, 31 participants including 8 countries) has been organized to engage such a project in ISS. Battery safety research in space environment must be developed based on the “Electrochemical Interface Processes for Space Battery and Devices” as WG even in JAXA.